

Microstructure characteristics of products in Ti–Si system via combustion synthesis reaction

Q. L. Guan · H. Y. Wang · S. L. Li ·
C. Liu · Q. C. Jiang

Received: 23 April 2008 / Accepted: 21 January 2009 / Published online: 11 February 2009
© Springer Science+Business Media, LLC 2009

Abstract The products of combustion synthesis reaction in Ti–Si system with molar ratios of Ti:Si = 3:1, 5:3, 5:4, 1:1, and 1:2 were investigated. The phase composition of products and degree of completion in the reaction considerably depend on the initial stoichiometric ratios of reactants. During the SHS reaction of Ti–Si system, the degree of completion follows the order of $5\text{Ti} + 3\text{Si} > \text{Ti} + \text{Si} > \text{Ti} + 2\text{Si} > 5\text{Ti} + 4\text{Si} > 3\text{Ti} + \text{Si}$. Besides, the microstructural morphology of Ti–Si compounds, i.e., TiSi_2 , TiSi , Ti_5Si_4 , and Ti_5Si_3 were also characterized in this study.

Introduction

Transition-metal silicides (Ti_xSi_y , Mo_xSi_y , Ta_xSi_y , and Nb_xSi_y , etc.) have received considerable attentions due to their unique properties [1–4] and the capability of extensive applications [5–7]. Particularly, in recent years, most research has been concentrated on Ti_5Si_3 and TiSi_2 , since they have a great potential for engineering application [8–11]. With the high melting temperature (2403 K), low density (4.32 g/cm^3), high hardness (11.3 GPa), good strength at elevated temperature, excellent creep resistance, and high oxidation resistance [2, 8, 12], Ti_5Si_3 has been considered as a promising candidate for high-temperature

structural material. Also, TiSi_2 is used popularly for the Si interconnects in the electronic industry because of its low electrical resistivity and high thermal stability [13].

Up to now, the fabrication methods of Ti_xSi_y can be generally summarized as the combustion synthesis [8, 9, 14], dynamic or shock-densification [15, 16], reaction hot pressing [17], and mechanical alloying [18, 19]. With the advantages of time and energy savings, combustion synthesis which is also referred as self-propagating high-temperature synthesis (SHS) has been recognized as an alternative route to the conventional methods of producing advanced materials [20–23], such as the Ti_xSi_y compounds.

Nowadays, considerable research has been focused on the fabrication techniques and reaction synthesis of Ti_xSi_y during SHS reaction. Anselmi-Tamburini et al. [24] have successfully combined the SHS technique with the mechanical alloying to fabricate the Ti_xSi_y compounds in different reactant stoichiometric ratios. Similarly, a comparative study on combustion synthesis of Ti_xSi_y was conducted by Yeh et al. [25]. The results are shown in Table 1. On the other hand, the reaction synthesis of Ti_5Si_3 in SHS reaction can be summarized as (i) the solid-state diffusion reaction [26], (ii) the liquid-state interaction [27], and (iii) the solid–liquid reaction (involving the dissolution-precipitation process) [8, 24, 25]. As for TiSi_2 , the formation process is divided as the solid-state [8] and the solid–liquid [14, 24] reaction. However, limited effort has been put in the study of microstructural morphology of Ti_xSi_y previously.

In this study, the microstructural evolution of Ti_xSi_y compounds in SHS reaction was studied with different starting compositions of molar ratios Ti:Si = 3:1, 5:4, 5:3, 1:1, and 1:2, respectively. This investigation was aimed at revealing the diversified morphologies of Ti_xSi_y compounds and phase composition of products in SHS reaction.

Q. L. Guan · H. Y. Wang · S. L. Li · C. Liu · Q. C. Jiang (✉)
Key Laboratory of Automobile Materials of Ministry
of Education, Department of Materials Science and Engineering,
Jilin University, Nanling Campus, No. 5988 Renmin Street,
Changchun 130025, People's Republic of China
e-mail: jiangqc@jlu.edu.cn

H. Y. Wang
e-mail: wanghy_jlu@yahoo.cn

Table 1 Summary of phase composition in combustion synthesis products with different stoichiometric ratios of reactants [24, 25]

Reactants Ti:Si	Combustion synthesis products	
	Anselmi-Tamburini et al. [24]	Yeh et al. [25]
1:2	TiSi ₂	TiSi ₂ , (TiSi, Si) ^a
1:1	TiSi, Ti ₅ Si ₃ , (TiSi ₂ , Ti ₅ Si ₄) ^a	TiSi, (Ti ₅ Si ₄ , TiSi ₂ , Ti) ^a
5:4	TiSi, Ti ₅ Si ₃ , (TiSi ₂ , Ti ₅ Si ₄) ^a	Ti ₅ Si ₄ , (TiSi, Ti) ^a
5:3	Ti ₅ Si ₃	Ti ₅ Si ₃
3:1	–	Ti ₅ Si ₃ , Ti

^a The product in brackets is the minor or trace phase

Experimental procedure

The starting materials used were the commercial powders of Ti (99.5% purity, ~38 μm) and Si (99.5% purity, ~15 μm). Titanium and silicon powders were used in different stoichiometric ratios corresponding to the phase diagram of Ti–Si system (Fig. 1), including Ti:Si = 3:1, 5:3, 5:4, 1:1, and 1:2. Powder blends with different starting compositions were mixed by ball-milling for 6 h to ensure homogeneity. Mixed powders were then cold-isostatically pressed into cylindrical compacts (22 mm in diameter) under pressures ranging from 70 to 75 MPa. The length of compact increased from ~11.3 to ~17.0 mm and the

green density of the compaction decreased from ~78 to ~39% with Ti:Si ratio decreasing from 3:1 to 1:2.

The combustion synthesis reaction was conducted in a combustion chamber under a protective atmosphere of industrial argon (99.9%). The compacts were placed on the graphite-flat which was fixed above a tungsten electrode and ignited by the arc heat. Microstructural characterization and phase analysis of the SHS products were investigated by using field emission scanning electron microscope (FESEM) (FEI-XL30, USA) equipped with energy-dispersive spectrum (EDS) (EDAX-Genesis 2000, USA). The chemical analyses are all performed on unpolished surfaces, and therefore the composition is the qualitative analysis rather than quantitative analysis. The average composition reported is calculated from six to ten grains. In addition, the samples were crushed into fine powders and analyzed for the phase composition by X-ray diffraction (XRD) using Cu Kα radiation (Model D/Max 2500PC Rigaku, Japan).

Results and discussion

Thermodynamic calculation

The potential reactions based on 1 mol reactant which could take place in Ti–Si system are conducted as follows:

Fig. 1 Phase diagram of Ti–Si system [28]

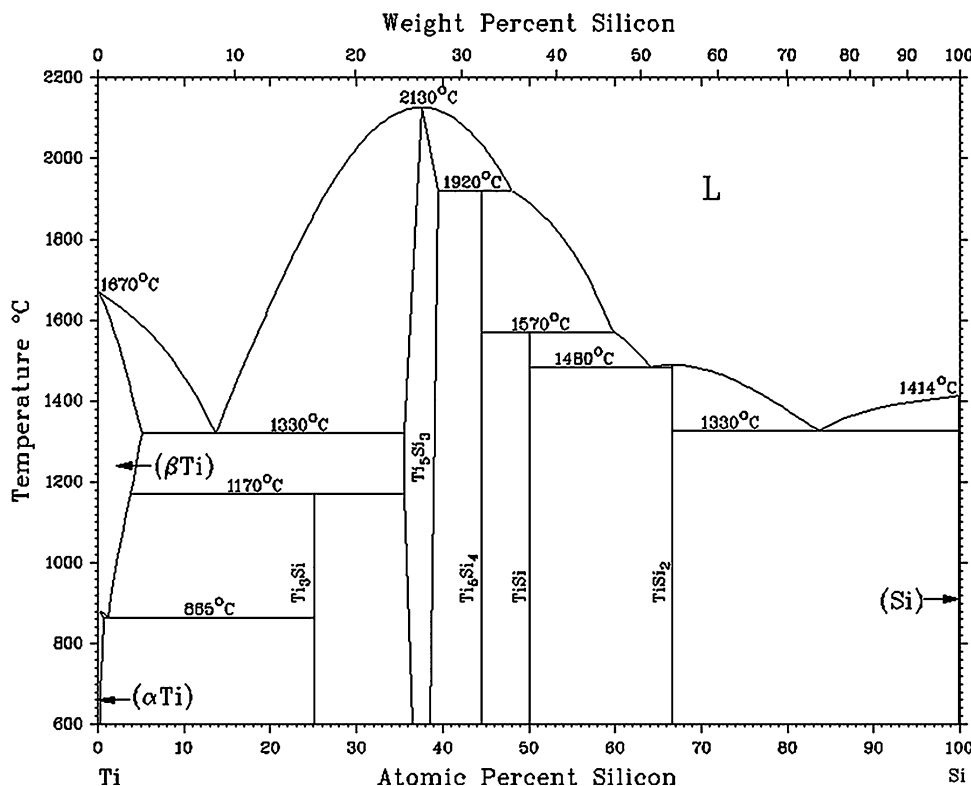




Figure 2 shows the theoretically calculated results of the change of the standard reaction enthalpy, ΔH^0 , as functions of temperature for Eqs. 1–3 according to the thermodynamics data [27, 29]. It can be observed that the changes in standard reaction enthalpy of the three reactions are all negative, which indicates that the above reactions are all exothermic in the calculated temperature ranges. Furthermore, the result reveals that ΔH_1^0 is more negative for the formation of Ti_5Si_3 than the other two possible compounds (TiSi and TiSi_2), which means Eq. 1 is the most exothermic among the three reactions. It is worth noting that the standard reaction enthalpy of Ti_5Si_4 cannot be calculated in this study, because the thermodynamic data are not available in the open literature. However, the result reported by Yeh et al. [25] showed that the peak temperature of the $5\text{Ti} + 4\text{Si}$ system researched up to $1420\text{ }^\circ\text{C}$, which was higher than the combustion temperatures of $\text{Ti} + \text{Si}$ ($\sim 1330\text{ }^\circ\text{C}$) and $\text{Ti} + 2\text{Si}$ ($\sim 1140\text{ }^\circ\text{C}$) systems. In addition, the front temperature ranges from 1380 to $1460\text{ }^\circ\text{C}$ in $5\text{Ti} + 3\text{Si}$ and $5\text{Ti} + 4\text{Si}$ systems.

The standard Gibbs free energy changes, ΔG^0 , of Ti–Si compounds based on 1 mol reactant were theoretically calculated by Zha et al. [30] in the study of Al–Ti–Si system. They proposed that the relatively thermodynamic stability of Ti_xSi_y compounds follows $\text{TiSi}_2 < \text{TiSi} < \text{Ti}_5\text{Si}_4 < \text{Ti}_5\text{Si}_3$, that is to say, $\Delta G^0(\text{Ti}_5\text{Si}_3) < \Delta G^0(\text{Ti}_5\text{Si}_4) < \Delta G^0(\text{TiSi}) < \Delta G^0(\text{TiSi}_2) < 0$. This result is consistent well with the sequence of phase transitions

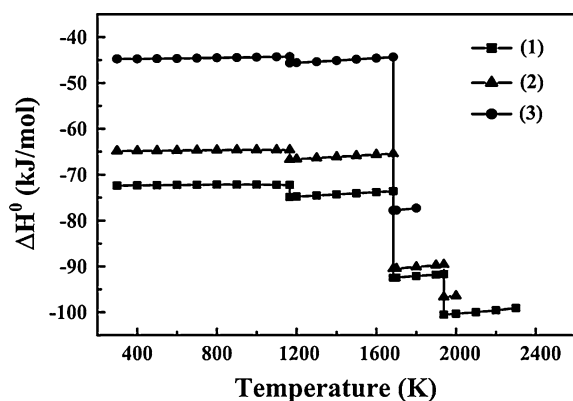


Fig. 2 Change of the standard reaction enthalpy, ΔH^0 , as temperature for Eqs. 1–3

reported by Thambukis and Munir [26, 31]. They presented that Ti_5Si_3 was formed during SHS process through a series of intermediate phase transitions, namely $\text{TiSi}_2 \rightarrow \text{TiSi} \rightarrow \text{Ti}_5\text{Si}_4 \rightarrow \text{Ti}_5\text{Si}_3$ [26, 31].

In conclusion, all the reactions that could take place in Ti–Si systems are thermodynamically favorable ($\Delta G^0 < 0$) and exothermic ($\Delta H^0 < 0$) in the given temperature range. The Ti_5Si_3 phase possesses higher thermodynamic stability than Ti_5Si_4 , TiSi , and TiSi_2 phases, implying that the latter phases, if they are formed, have a tendency to transform to the former one at elevated temperature.

XRD analysis

In this study, it is worth noting that the combustion reaction of $\text{Ti} + 2\text{Si}$ compact is hardly ignited without any preheating and going to be self-extinguished right after the ignition with significantly slow flam-front velocity. This phenomenon is quite different from that of other compacts in the combustion synthesis experimental process, mainly due to the fact that the exothermicity of reaction front of TiSi_2 formation (Fig. 2) is too low to maintain the SHS reaction [25]. The poor compactibility and relatively low degree of compaction also inhibit the SHS reaction of $\text{Ti} + 2\text{Si}$ system. Therefore, in this study, the compact of $\text{Ti} + 2\text{Si}$ system was preheated to $\sim 400\text{ }^\circ\text{C}$ in order to facilitate the initiation of SHS reaction.

Figure 3 shows XRD patterns of the reaction products in Ti–Si system with Ti:Si molar ratios of (a) 3:1, (b) 5:3, (c) 5:4, (d) 1:1, and (e) 1:2, respectively. It can be seen that the degree of completion and phase composition of SHS reaction products considerably depend on the stoichiometric ratios of reactants. Obviously, the products from the $3\text{Ti} + \text{Si}$ system mainly consist of Ti_5Si_3 and unreacted Ti phases (Fig. 3a) rather than expected single-phase Ti_3Si , suggesting a poor degree of completion of SHS reaction. However, complete conversion yielding a single-phase Ti_5Si_3 is achieved in $5\text{Ti} + 3\text{Si}$ system (Fig. 3b). In $5\text{Ti} + 4\text{Si}$ system, the Ti_5Si_4 , Ti_5Si_3 , and TiSi phases are identified by XRD in final products (Fig. 3c). The reaction of $\text{Ti} + \text{Si}$ system generates a multiphase products consisting of major TiSi , along with minor TiSi_2 and Ti_5Si_4 phases (Fig. 3d). For $\text{Ti} + 2\text{Si}$ system, a large amount of TiSi_2 combining with little TiSi and residual Si is detected in final products (Fig. 3e).

According to XRD results, it is concluded that the degree of completion in the SHS reaction of Ti–Si system is ordered by $5\text{Ti} + 3\text{Si} > \text{Ti} + \text{Si} > \text{Ti} + 2\text{Si} > 5\text{Ti} + 4\text{Si} > 3\text{Ti} + \text{Si}$, which differs from that of the aforementioned thermodynamic stability of Ti_xSi_y compounds. It is the reaction kinetics that determines the phase composition of products and degree of completion in the SHS reaction.

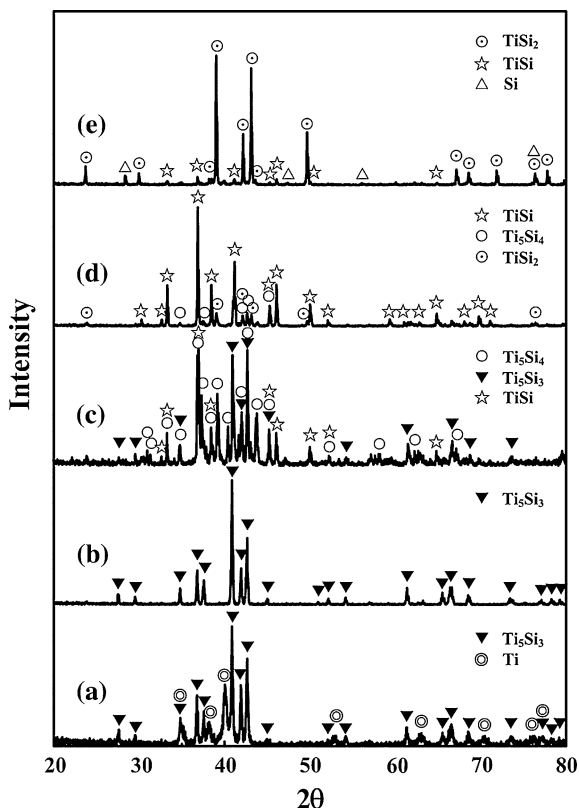


Fig. 3 XRD patterns of SHS reaction products in Ti–Si system synthesized by compacts with different Ti:Si molar ratios of (a) 3:1, (b) 5:3, (c) 5:4, (d) 1:1, and (e) 1:2, respectively

In this study, the phase composition of products in Ti + 2Si, 5Ti + 3Si, and 3Ti + Si systems is consistent well with that reported in the literature [25], while difference still exists in products of other systems (Ti + Si and 5Ti + 4Si). Comparing with the literature [24], however, more difference is present in the products of Ti + Si, 5Ti + 4Si, and Ti + 2Si systems. It can be attributed to the variety of raw particle size and experimental conditions (e.g., the ignition method, degree of compaction, and fabrication technique, etc.), which considerably influence the reaction route and degree of completion.

Microstructure analysis

Ti + 2Si system

Figure 4 shows the typical FESEM microstructure and backscattered electron image of the products in Ti + 2Si system. It can be seen that the morphology of large grain exhibits a cobblestone-like shape with the size of ~10 to ~40 μm (Fig. 4a). According to EDS analysis, the average composition of the large grain is 31 at.% Ti and 69 at.% Si. Combining with XRD analysis, the $TiSi_2$ is the dominant phase in the final products of Ti + 2Si system (Fig. 3e).

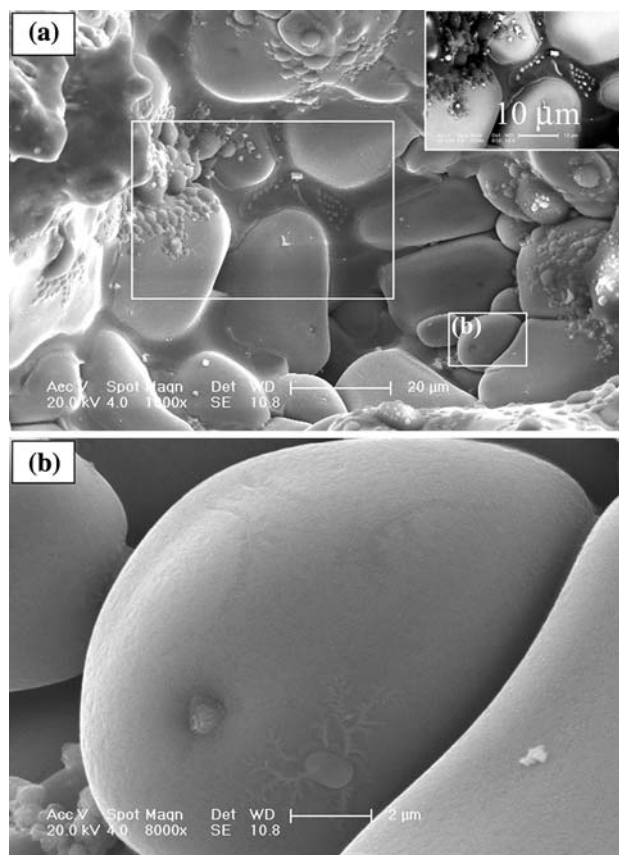


Fig. 4 Typical FESEM microstructure of the products in combustion synthesis reaction of Ti + 2Si system (the inset is the backscattered electron microscopy of the central frame), and **b** is the local magnification of the selected area in (a)

Therefore the smooth particulates correspond to the $TiSi_2$ phase. The inset of Fig. 4a is the back-scattered electron microscopy of the central frame. Obviously, the composition of grain boundaries is quite different from that of the $TiSi_2$ phase. It is identified as a Si-rich phase with a small amount of Ti dissolving.

Yeh et al. [25] reported that the formation process of $TiSi_2$ synthesized by the compact with a high degree of compaction (60%) was governed by the solid-state interaction due to the low combustion temperature. Anselmi-Tamburini et al. [24] argued that the presence of round-shaped $TiSi_2$ was characterized by the dissolution of Ti into Si-rich melts followed by the precipitation of the $TiSi_2$ phase, mainly due to the effect of mechanical activated technique on the SHS reaction. In this study, the reaction synthesis of $TiSi_2$ was characterized by the dissolution-precipitation process, owing to the influence of preheating on the compact. Moreover, the dissolution-precipitation process can be further confirmed by the presence of residual liquids in grain boundaries (inset of Fig. 4a), nearly spherical morphology and smooth surface of particulates (Fig. 4b).

Up to now, the report about the morphology of TiSi_2 synthesized by SHS is rather limited. Tomoshige et al. [32] observed that TiSi_2 grains, which were fabricated by combing SHS with high-temperature-shock compaction technique, exhibited coarse tetragonal and rod-like shape with the average size of $\sim 7 \mu\text{m}$. In addition, Vardumyan et al. [33] fabricated the columnar TiSi_2 with the size of $10 \mu\text{m}$ in length and $0.1\text{--}1 \mu\text{m}$ in diameter by using foaming agents under SHS condition.

Ti + Si system

Figure 5 shows the typical FESEM microstructure of the products in Ti + Si system. It can be observed that large volumes of particulates with white shiny appearance are formed in the products. The small particulates consist of 52 at.% Ti and 48 at.% Si, identified by EDS. Based on XRD results, TiSi is the dominant phase in SHS products of Ti + Si system (Fig. 3d). Hence, it can be concluded that the small shiny particulates with the size of ~ 1 to $3 \mu\text{m}$ are TiSi phase. From the local magnification (Fig. 5b), it is believed that the formation of TiSi can be characterized by the solution-precipitation process from the liquids.

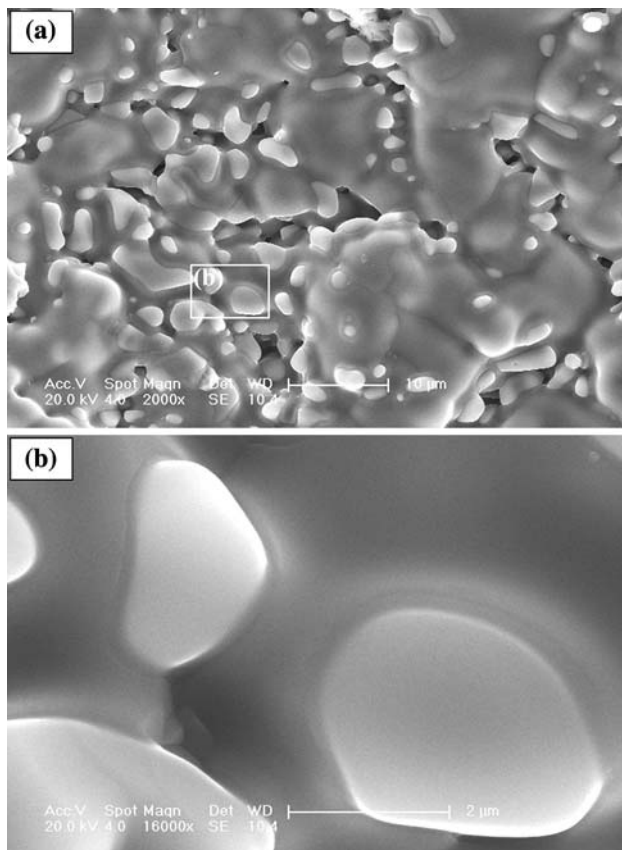


Fig. 5 Typical FESEM microstructure of the products in combustion synthesis reaction of Ti + Si system, and **b** is the local magnification of the selected area in **(a)**

5Ti + 4Si system

Figure 6a–d shows the typical FESEM microstructures in pores and fractured surface of the products in 5Ti + 4Si system. Figure 6b and d illustrates the morphologies from different pores, respectively. Combing with XRD analysis, both Ti_5Si_3 and Ti_5Si_4 phases can be detected in products of 5Ti + 4Si system. According to EDS results, the large grains ($\sim 10\text{--}40 \mu\text{m}$) consist of 57 at.% Ti and 43 at.% Si; whereas the small particulates ($\sim 5 \mu\text{m}$) existing in the grain boundaries consist of 56 at.% Ti and 44 at.% Si (Fig. 6b). Thus all the particulates are identified as Ti_5Si_4 phase (Fig. 6b).

Figure 6c reveals a typical microstructure of the fracture surface in the products. The tiny particulates in size of $\sim 3 \mu\text{m}$ are identified as Ti_5Si_3 phase, as shown in the inset of Fig. 6c. Figure 6d shows a long thin tubular phase with a hollow hexagonal section, which generally locates in the pores of products (Fig. 6a). Based on EDS analysis, the composition of the tubular phase is 62 at.% Ti and 38 at.% Si; therefore, it is also identified as Ti_5Si_3 . The reason why Ti_5Si_3 grains exhibit the tubular shape in the pores could not be clarified in this study.

5Ti + 3Si and 3Ti + Si systems

Figure 7a, b and c, d represents the typical FESEM microstructure of the products in 5Ti + 3Si and 3Ti + Si systems, respectively. It can be seen that most of Ti_5Si_3 grains exhibit sintered morphology with coarse appearance (Fig. 7a). Furthermore, the trans- and inter-granular microcracks are also clearly observed (Fig. 7b), which may account for the great anisotropy of coefficient of thermal expansion of Ti_5Si_3 [9] and the high thermal residual stress in products.

Combined with XRD results, the phase composition of products in 3Ti + Si system is not equivalent to the designed composition (Fig. 3a); that is to say, no Ti_3Si phase is formed in the SHS reaction of 3Ti + Si system. In contrast, Ti_5Si_3 and residual Ti are detected in the final products. The viewpoint of Yeh et al. [25] is that Ti_3Si might be kinetically unfavorable because no trace of Ti_3Si was detected in the SHS reaction product from any test sample. Also, the presence of large primary precipitates of Ti_5Si_3 contributed to a reduction in the kinetics of Ti_3Si formation [34]. However, a large amount of Ti_3Si phase was fabricated by Romos et al. [34] through arc-melted Ti–13.5Si alloys and a heat treatment at $1100 \text{ }^\circ\text{C}$, confirming its existence in Ti–Si alloys containing low interstitial contents.

In this study, the particulates surrounded by large numbers of Ti-rich phase are identified as Ti_5Si_3 (Fig. 7c) by combining EDS with XRD (Fig. 3a). The local magnification of the selected area clearly shows that the

Fig. 6 Typical FESEM microstructure of the products in combustion synthesis reaction of $5\text{Ti} + 4\text{Si}$ system, **a** low magnification and **b–d** are the high magnification of the frames in **(a)** (the inset is local magnification of the selected area)

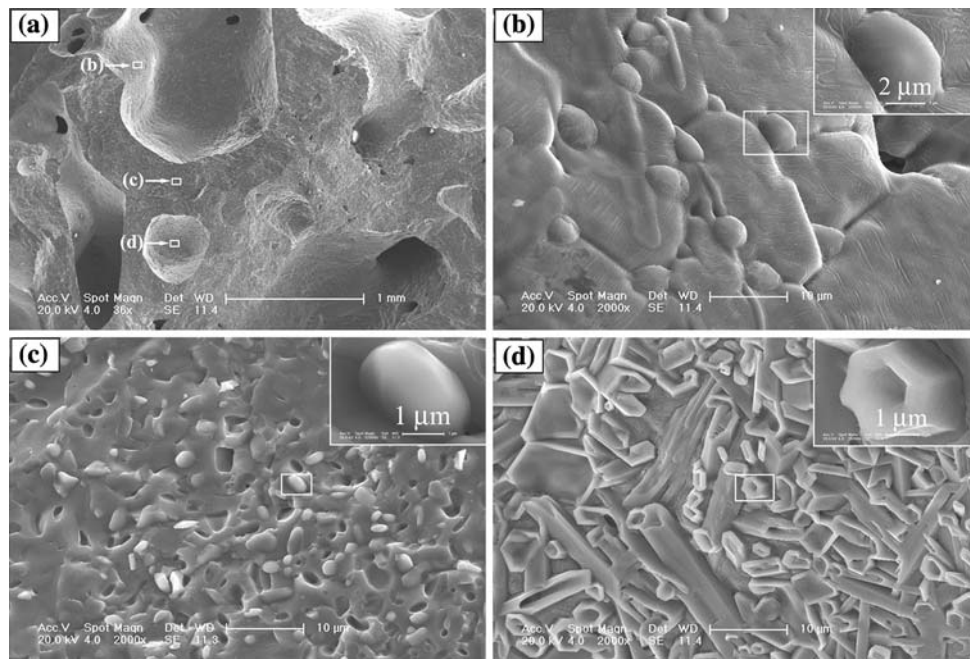
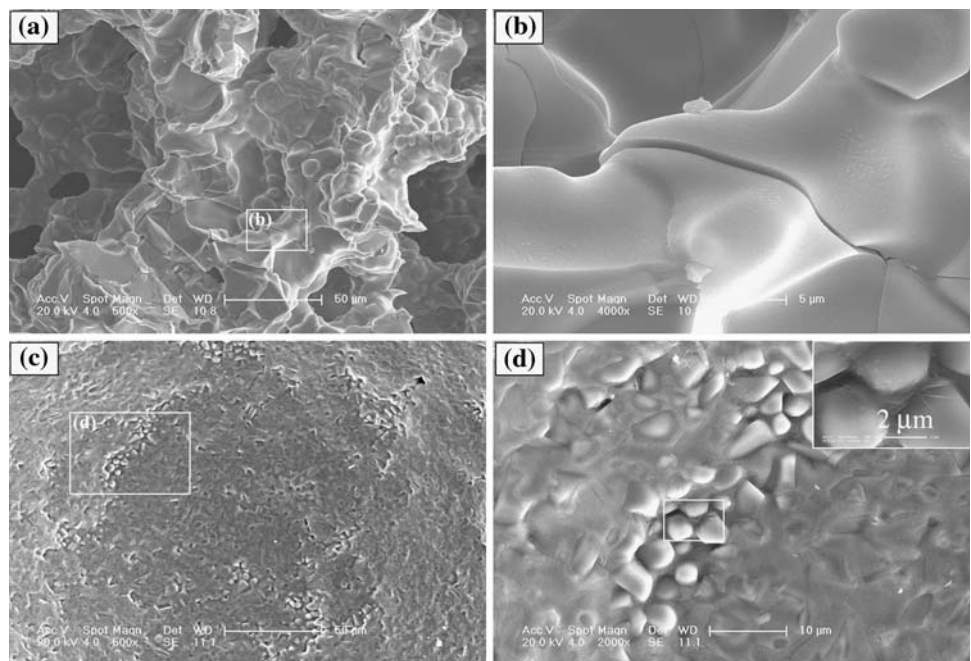


Fig. 7 Typical FESEM microstructure of the products in combustion synthesis reaction of **a** $5\text{Ti} + 3\text{Si}$ system, **b** high magnification of the selected areas in **(a)**, **c** $3\text{Ti} + \text{Si}$ system, and **d** high magnification of the selected areas in **(c)** (the inset is local magnification of the selected area)



morphology of Ti_5Si_3 synthesized in $3\text{Ti} + \text{Si}$ system is nearly spherical in the size of $\sim 2 \mu\text{m}$ (the inset of Fig. 7d).

Conclusions

The products of combustion synthesis reaction in Ti–Si system with molar ratios of $\text{Ti}:\text{Si} = 3:1, 5:3, 5:4, 1:1,$ and $1:2$ were investigated. The phase composition and degree of completion of SHS reaction considerably depend on the stoichiometric ratios of reactants. In $5\text{Ti} + 3\text{Si}$, $\text{Ti} + \text{Si}$,

and $\text{Ti} + 2\text{Si}$ systems, the dominant phase in products agreed well with the designed one. In $5\text{Ti} + 4\text{Si}$ system, the products consisted of Ti_5Si_4 , Ti_5Si_3 , and TiSi phases, rather than the desired monolithic phase. In $\text{Ti} + 3\text{Si}$ system, however, no Ti_3Si was formed and the products only consisted of Ti_5Si_3 and residual Ti phases. Thus, the degree of completion of SHS reaction in Ti–Si systems follows the order of $5\text{Ti} + 3\text{Si} > \text{Ti} + \text{Si} > \text{Ti} + 2\text{Si} > 5\text{Ti} + 4\text{Si} > 3\text{Ti} + \text{Si}$. Meanwhile, the microstructural morphology of Ti–Si compounds, i.e., TiSi_2 , TiSi , Ti_5Si_4 , and Ti_5Si_3 are characterized, respectively, in this study.

Acknowledgements Financial support from the National Science Foundation of China (Nos. 50671044 and 50531030) is gratefully acknowledged. Partial financial support comes from the Program for New Century Excellent Talents (No. 06-0308) and the Science and Technology Development Planning of Jilin Province (20070110) as well as the Project 985-Automotive Engineering of Jilin University.

References

1. Meschter PJ, Schwartz DS (1989) *JOM* 41:52
2. Shah DM, Berczik D, Anton DL, Hecht R (1992) *Mater Sci Eng A* 155:45
3. Petrovic JJ (2000) *Intermetallics* 8:1175
4. Yeh CL, Chen WH (2007) *J Alloys Compd* 439:59
5. Stoloff NS (1999) *Mater Sci Eng A* 216:169
6. Murarka SP (1995) *Intermetallics* 3:173
7. Handtrack D, Sauer C, Kieback B (2008) *J Mater Sci* 43:671. doi: [10.1007/s10853-007-2160-2](https://doi.org/10.1007/s10853-007-2160-2)
8. Yeh CL, Chen WH, Hsu CC (2007) *J Alloys Compd* 432:90
9. Riley DP, Oliver CP, Kisi EH (2006) *Intermetallics* 14:33
10. Umakoshi Y, Nakashima T (1992) *Scr Metall* 66:317
11. Rosenkranz R, Frommeyer G, Smarsly W (1992) *Mater Sci Eng A* 152:288
12. Sandwick T, Rajan K (1990) *J Electron Mater* 19:1193
13. Murarka SP (1983) *Silicides for VLSI applications*. Academic Press, Orlando
14. Sarkisyan AR, Sarkisyan MM, Kharatyan SL (1993) *J Eng Phys Thermophys* 65:1012
15. Namjoshi SA, Thadhani NN (1990) *Scr Mater* 40:1347
16. Namjoshi SA, Thadhani NN (2000) *Metall Mater Trans B* 31:307
17. Mitra R (1998) *Metall Trans A* 29:1629
18. Lee YS, Lee SM (2007) *Mater Sci Eng A* 449:1099
19. Yen BK, Aizawa T (1998) *J Am Ceram Soc* 81:1953
20. Munir ZA, Anselmi-Tamburini U (1989) *Mater Sci Rep* 3:277
21. Merzhanov AG (1994) *Combust Sci Technol* 98:307
22. Moore JJ, Feng HJ (1995) *Prog Mater Sci* 39:243
23. Mossino P (2004) *Ceram Int* 30:311
24. Anselmi-Tamburini U, Maglia F, Spinolo G, Doppiu S, Monagheddu M, Cocco G (2000) *J Mater Synth Process* 8:377
25. Yeh CL, Wang HJ, Chen WH (2008) *J Alloys Compd* 450:200
26. Trambukis J, Munir ZA (1990) *J Am Ceram Soc* 73:1240
27. Liang YJ, Chen YC (1993) *Data handbook of mineral thermodynamics*. Northeastern Press, China
28. Massalski TB (1990) *Binary alloy phase diagrams*, 2nd edn. ASM International, Materials Parks, OH, USA
29. Brain I (1995) *Thermochemical data of pure substance*, 3rd edn. Wiley-VCH Verlag GmbH, Weinheim
30. Zha M, Wang HY, Li ST, Li SL, Guan QL, Jiang QC (2007) *Mater Chem Phys*. doi: [10.1016/j.matchemphys.2008.10.024](https://doi.org/10.1016/j.matchemphys.2008.10.024)
31. Du YJ, Rao KP, Chung JCY, Han XD (2000) *Metall Mater Trans A* 31:763
32. Tomoshige R, Goto T, Matsushita T, Imamura K, Chiba A, Fujita M (1999) *J Mater Process Technol* 85:100
33. Vardumyan LE, Khachatryan HL, Harutyunyan AB, Kharatyan SL (2008) *J Alloys Compd* 454:389
34. Ramos AS, Nunes CA, Coelho GC (2006) *Mater Charact* 56:107